TRANSPORTATION OF SOLID PARTICLES

IN A GAS FLOW STREAM

By

KIRK EWELL BOATRIGHT

Bachelor of Science

Oklahoma State University

Stillwater, Oklahoma

1959

Submitted to the faculty of the Graduate School of
The Oklahoma State University
in partial fulfillment of the requirements
for the degree of
MASTER OF SCIENCE
August, 1960

TRANSPORTATION OF SOLID PARTICLES IN A GAS FLOW STREAM

Thesis Approved:

Glen W. Bennett
Thesis Adviser

Ladislaus J. Fila

Dean of the Graduate School

PREFACE

The purpose of this thesis was to determine a correlation between the pressure drop and the properties of the 2-phase flow system and to design and select the apparatus with which the necessary experimental data can be obtained. The selection of a method for injection of the solid particles into the flow stream required considerable study. A system must be used which will provide a uniform flow into the test section and a solid storage capacity sufficient to maintain this flow throughout the test run. Minimum obstruction of the gas flow stream is necessary. The following types of systems were considered: (1) auger, (2) variable speed gear, (3) forced air injection, and (4) free-flow hopper. It was found that the free-flow hopper system was adequate and caused negligible fluctuation in pressure readings. It is necessary that the injection openings into the flow stream be completely covered by solid particles if flow is to be uniform.

The apparatus was assembled and the desired correlation obtained using air and water as the flow components.

This study has been performed through a graduate fellowship sponsored by the Pan American Petroleum Corporation. Thanks is given for their enthusiasm in engineering education and the financial assistance awarded for this research project.

I express my appreciation to my graduate adviser, Dr. Glen W. Zumwalt, for his interest in the project and constructive criticisms of the rough draft. Recognition is due Dr. J. H. Boggs for his suggestions and interest, Professor A. G. Comer for his assistance and advice, Mr. Tim Tarleton for his aid in making the test runs, and Mr. John McCandless and Mr. George Cooper for their suggestions, assistance, and patience while the research equipment was being assembled. I thank Mrs. Mildred Avery for her assistance in typing and assembling this final report.

To my parents, Mr. and Mrs. E. A. Boatright, who have given guidance and support throughout my college years, I dedicate this paper.

TABLE OF CONTENTS

LIST OF TABLES

LIST OF ILLUSTRATIONS

SYMBOLS AND ABBREVIATIONS

A	Area of flow (ft^2)
A_p	Projected area of the particle in the direction of motion
C_D	Drag Coefficient expressed as a function of the Reynolds number
D	Diameter of the pipe (ft)
D_p	Diameter of the particle
F	Net gravitational force on the particle
g	Local acceleration due to gravity
g_c	32.174 $(lb_m\text{-}ft)/(lb_f\text{-}sec^2)$
K_w	Factor which considers wall effect in U_T calculations
N_R	Reynolds number
P	Absolute pressure
ΔP	Pressure drop in the test section for 2-phase flow
ΔP_g	Pressure drop in the test section for air flowing alone
Q	Flow rate of gas (ft^3/min)
Q_{gs}	Rotameter reading for air flowing alone (cubic ft/min. at 14.696 psia and 100°F)
Q_{ga}	Q_{gs} corrected for conditions existing during flow of air only (cubic ft/min. at T_a and P_a)
Q_{2s}	Rotameter reading for 2-phase flow (cubic ft/min. at 14.696 psia and 100°F)
Q_{2a}	Q_{2s} corrected for conditions existing during flow of air only (cubic ft/min. at T_a and P_a)
Q_{2f}	Q_{2s} corrected for conditions existing during 2-phase flow (cubic ft/min. at T and P)
R	Gas constant $(ft\text{-}lb_f)/(lb_m\text{-}^oR)$
T	Absolute temperature (^oR)

Time	Time elapsed during the test run (min.)
U	Particle velocity
U_T	Terminal velocity of the particle
V	Volume of the particle
v	Velocity of gas flow neglecting the effect of particles in the flow stream (ft/sec.)
W	Weight of the particles (lb)
$\dot{w}_g$	Weight rate of gas flow (lb/min.)
$\dot{w}_p$	Weight rate of particle flow (lb/min.)
z	Gas compressibility factor
ρ_g	Mass density of the gas (lb_f-sec^2/ft^4)
ρ_p	Mass density of the particle (lb_f-sec^2/ft^4)
μ	Absolute viscosity of the gas (lb_f-sec/ft^2)
lb_f	Pound force unit
lb_m	Pound mass unit
I.D.	Inside diameter
O.D.	Outside diameter
^oR	Degrees Rankine

1st subscripts:

g = gas flow only

2 = 2-phase flow

2nd subscripts:

s = measured at standard conditions of 14.696 psia and 100°F

a = measured at conditions of air flow only (T_a and P_a)

f = measured at conditions of 2-phase flow (T and P)

CHAPTER I

INTRODUCTION

The gas flow stream has been applied, by many industries in recent years, to the problem of transportation of solid particles. The petroleum and grain industries yield examples of such applications. In the petroleum industry, air is used as a drilling fluid to transport the drill cuttings from the well. The grain industry transports small grains by introducing them into an air stream. The resulting 2-phase flow stream has many interesting properties and characteristics.

As a result of interest shown in this field, a research project was undertaken which was sponsored by the Pan American Petroleum Corporation. The purpose of the project was to design and assemble equipment in the Mechanical Engineering Laboratory of Oklahoma State University for the measurement of properties of the vertically upward, isothermal, 2-phase flow system; to attempt to correlate the ratio of pressure drops, $(\Delta P/\Delta P_g)$, to the properties, $\dot{w}_p$, $\dot{w}_g$, ρ_g, ρ_p, and $(N_R)_g$; to analyze the results. The test results are presented in this report.

CHAPTER II

REVIEW OF THE LITERATURE

Many studies have been made to determine the flow characteristics of one-phase, two-phase, and three-phase flow. One-phase flow is gas or liquid flowing alone; two-phase flow is a flow stream of gas-liquid, gas-solid, or liquid-solid mixtures; three-phase flow is a flow stream of a gas-liquid-solid mixture. Since the purpose of this report is the discussion of the transportation of solid particles in a gas flow stream, this literature review summarizes only the results of the major studies of gas-solid, two-phase flow.

It is necessary to evaluate the properties of the system when approaching any two-phase flow problem. The type of flow (viscous or turbulent), the properties of the transporting medium, and the characteristics of the flow boundaries must be determined. Many problems have been encountered in these determinations. Several investigators have attempted to consider the two-phase system as being homogeneous and to correlate pressure drops on this basis. However, the determination of the properties of this homogeneous fluid is difficult and makes this method unpopular. Viscosity is an example of such a property.

J. Happel (1) developed a method for determination of the viscosity of suspensions of uniform spheres. This mathematical development

is based on the steady-state Stokes-Navier equations of motion omitting the inertia terms. The disturbance due to each sphere is assumed to be confined to a frictionless envelope surrounding it similar to a stream tube for flow inside ducts. The relationship obtained by this method is in good agreement with existing data.

The terminal velocity of a particle is the maximum velocity attained in free fall in a fluid medium. In order to transport particles vertically in a fluid stream, velocities in excess of the terminal velocities of the particles are required. Ideally, when the fluid velocity exceeds the terminal velocity of the particle, the particle will move upward with a velocity equal to the difference between the fluid and terminal velocities.

The "choking" velocity, and for practical purposes, the "slip", is essentially the minimum transport velocity necessary to convey the solids.

H. O. Croft (2) presented equations for determination of the terminal velocity of particles based on the assumption that the net gravity force on the particle is equal to the fluid resisting force acting on the particle.

If the net gravity force = $F = V_g(\rho_p - \rho)$ where

F = net gravitational force

V = volume of the particle

g = local acceleration due to gravity

$\rho_p = W/g$ = mass density of the particle

W = Weight of the particle

ρ_g = mass density of the fluid

and the fluid resisting force = $R = (C_D/2)A_p U^2 \rho_g$ where

R = total resistance of the fluid to particle motion

A_p = projected area of the particle in the direction of motion

U = particle velocity

ρ_g = mass density of the fluid

C_D = drag coefficient expressed as a function of the Reynolds number, N_R

a relation for particle terminal velocity, U_T, can be found by letting $F = R$ and solving for U. The result is

$$U_T = \sqrt{(2Vg/C_D A_p)\ [(\rho_p - \rho_g)/\rho_g]}\ .$$

For the determination of C_D for spherical particles, see Table I.

The wall effect on the value of U_T becomes important when the ratio of the diameter of the particle to the diameter of the pipe exceeds 0.2. This effect can be considered by dividing U_T as calculated from the equation, by the factor K_w.

For values of the diameter ratios less than 0.1,

$$K_w = 1.0 + 2.1(D_p/D).$$

For diameter ratios ranging from 0.13 to 0.97 and values of N_R from 0.000015 to 6.9,

$$K_w = [1.0 - (D_p/D)]^{-2.5}$$

where

D_p = diameter of the particle

D = diameter of the pipe

N_R = Reynolds number.

TABLE I

DRAG COEFFICIENTS (C_D) FOR SPHERICAL PARTICLES

N_R	C_D
0.1	$24/N_R$
0.1 to 2.0	Approx. $(24/N_R)$
2 to 1000	$18.5/(N_R)^{0.6}$
1000 to 200,000	Approx. 0.44

TABLE II

VISCOSITY AND DENSITY OF AIR AND WATER

FLUID	TEMPERATURE °F	VISCOSITY (cp)	DENSITY (lb_m/ft^3)
Air	70	0.0181	0.0749
Water	70	0.981	62.3

The information on wall effect is generally used for streamline flow. It should be noted that the terminal velocity relationship given here is for solid particles in a gas flow stream of one particular gas.

Figure 1 shows terminal settling velocities of spherical particles of different densities settling in air and water at 70°F under the action of gravity. In this figure, numbers on the curves represent true (not bulk or apparent) specific gravity of particles referred to water at 4°C. The physical properties used in obtaining the curves are shown in Table II.

It should be noted that the treatment presented by Croft considers the individual particle in an unbounded fluid stream.

The determination of pressure drops in flow systems is important. G. E. Alves (3) predicted that the components of the total pressure drop in the gas-solid system should be as follows:

1. That required to accelerate the gas to the carrying velocity
2. That required to overcome the friction of the gas on the pipe walls
3. That required to supply the loss of momentum of the gas in
    (a) accelerating the solids
    (b) keeping the solids in suspension
4. That required to support the gas
5. That required to support the solids.

An important paper was presented by O. H. Hariu and M. C. Molstad (4) on the pressure drop in vertical 0.267 and 0.532 inch

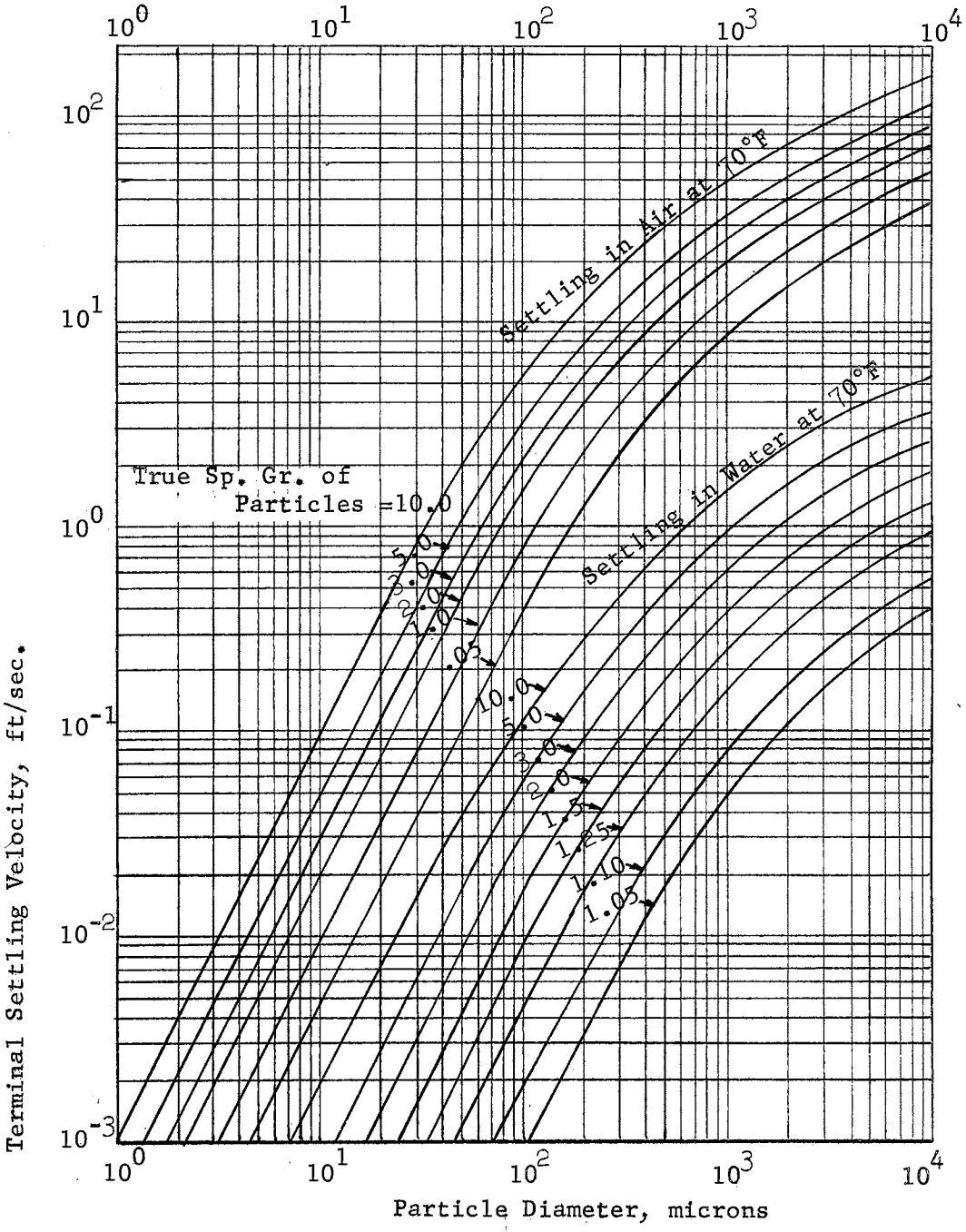

Figure 1. Terminal Velocity vs. Particle Diameter

inside diameter glass tubes with air as the fluid medium. Closely sized sand (28- to 35-, 35- to 48-, 48- to 60-, and 60- to 80- mesh Tyler) and both ground and spherical silica-alumina cracking catalyst were used. Solids circulation rates ranged from 2 to 54 pounds per second per square foot at various constant air rates ranging from 0.9 to 3.0 pounds per second per square foot, equivalent to 12 to 40 feet per second. Calculations of the average particle velocity, slip velocity and pressure drop could be made since direct measurements of the dispersed solids density were taken.

The paper presented analytical expressions to determine the pressure drops, horsepower output, horsepower input, mechanical efficiency, and the slip factor. Graphs were introduced to correlate the experimental work with the analytical study. A description of the apparatus along with operating procedure was contained in the paper.

R. H. Wilhelm and M. Kwauk (5) reported on the fluidization of solid particles by means of air and water in 3-inch and 6-inch diameter columns. Spherical and uniformly sized particles of sand, glass, silicate catalyst, and lead shot, ranging in size from 5mm to 0.3 mm in diameter, and in density from 1.125 to 10.792 gm/cc. were used. Pressure drop, fraction void, and velocity were measured and then correlated by means of four dimensionless groups.

The paper deals primarily with fluidized beds and presents experimental measurements on fluidization from a quiescent bed to the maximum possible degree of expansion, with water and with air.

Allen Hazen, E. D. Hardy, and Nora Stanton Blatch (6) made early investigations on the transportation of sand in dredges. The tests dealt primarily with pressure loss determinations and revealed that for horizontal pipes, the pressure loss due to carrying the sand is quite significant at low velocities. The loss is reduced at higher velocities. The results of their experiments lead to the assumption that for flow of solids and gas in vertical pipes, when the velocity is great enough to lift the particles they will be in fluidized form thus creating a pressure drop of some constant value in excess of that required to pump only the gas. No data, however,was taken for vertical flow.

John L. Alden (7) experimented with low pressure pneumatic conveying of solids in air. He concluded that dense materials require less air per pound than do lighter and bulkier substances. It was found that from 35 to 50 cubic feet of air per pound of solid would carry practically any material which can be conveyed.

S. L. Soo, H. K. Ihrig, Jr., and A. F. El Kouh (8) presented a paper which discusses the determination of the turbulence characteristics of both the solid and fluid phases of a two-phase (solid suspended and conveyed in a gas) flow stream. The stream is a fully developed turbulent air stream flowing horizontally and transporting spherical glass beads of close size range. The turbulence of the fluid phase and of the solid particles was determined by using a tracer-diffusion technique and a photo-optical technique respectively.

Their experiments showed that:

1. For a two-phase turbulent stream of the loading from 0.01 to 0.06 lb of solid per lb of air and particle size below 250-micron diameter, the stream turbulence is not significantly affected by the presence of the particles.
2. The particle motion is nonisotropic, even where the stream motion is nearly isotropic, mainly due to gravity and wall effects.
3. The intensity of particle motion is greatly affected by the distribution of stream intensity in the duct.
4. The probability of particle-stream encounter has a significant effect on the particle diffusivity, which, in the cases studied is of the order of 10^{-2} of the eddy diffusivity of the stream.
5. The particle Reynolds number of the cases investigated is, in all cases, below 10; hence the Stokes approximation of drag is a reasonable one.

One of the most valuable contributions to the literature on transportation of solids in a gas flow stream was presented by Frederick A. Zenz (9). The paper gives the results of a series of experiments to determine the flow characteristics of particle-fluid mixtures having a large particle-to-fluid weight ratio, essentially a fluidized bed. Tests were run for vertical and horizontal flow with air as the fluid medium and solid particle size from 0.0066 to 0.066 inch in diameter. The test section was a 1.75-inch I. D.

lucite tube.

Figure 2 shows the results of the flow tests. In the vertical flow system at velocities below that at which the curves show minimum pressure drops, the particle velocities decrease and there is a considerable increase in hold up of particles in the tube. The solids apparently continue to flow through the increasingly dense mass of slowly moving particles floating in the tube. The increased pressure drop is due to the weight of material hold up that slowly ascends in the tube. With a further reduction in air velocity, the particles became extremely turbulent and the hold up of material eventually caused slugging to take place. Slugging or erratic flow is indicated in the figure by the dashed lines. These features appear in the transition region separating true 2-phase flow and fluidized bed flow.

The curves for horizontal flow are shown in the lower part of Figure 2. The breaks in the curves are due to the settling out of particles in the tube. More particles settled out at velocities less than the settling velocity and filled the tube with a deep layer of particles causing a rapid increase in pressure drop. A comparison of the curves for horizontal and vertical flow indicates that choking in vertical flow occurs at the same velocity as settling in horizontal flow.

Many additional articles discussing the gas-solid flow system are available for study. Only a few have been summarized in this review to acquaint the reader with the background material for the

ϵ = Fraction voids in bed of solids, cu. ft./cu. ft.

W = Weight rate, lbs. of solids transported/(sec.)(sq. ft. of pipe cross section)

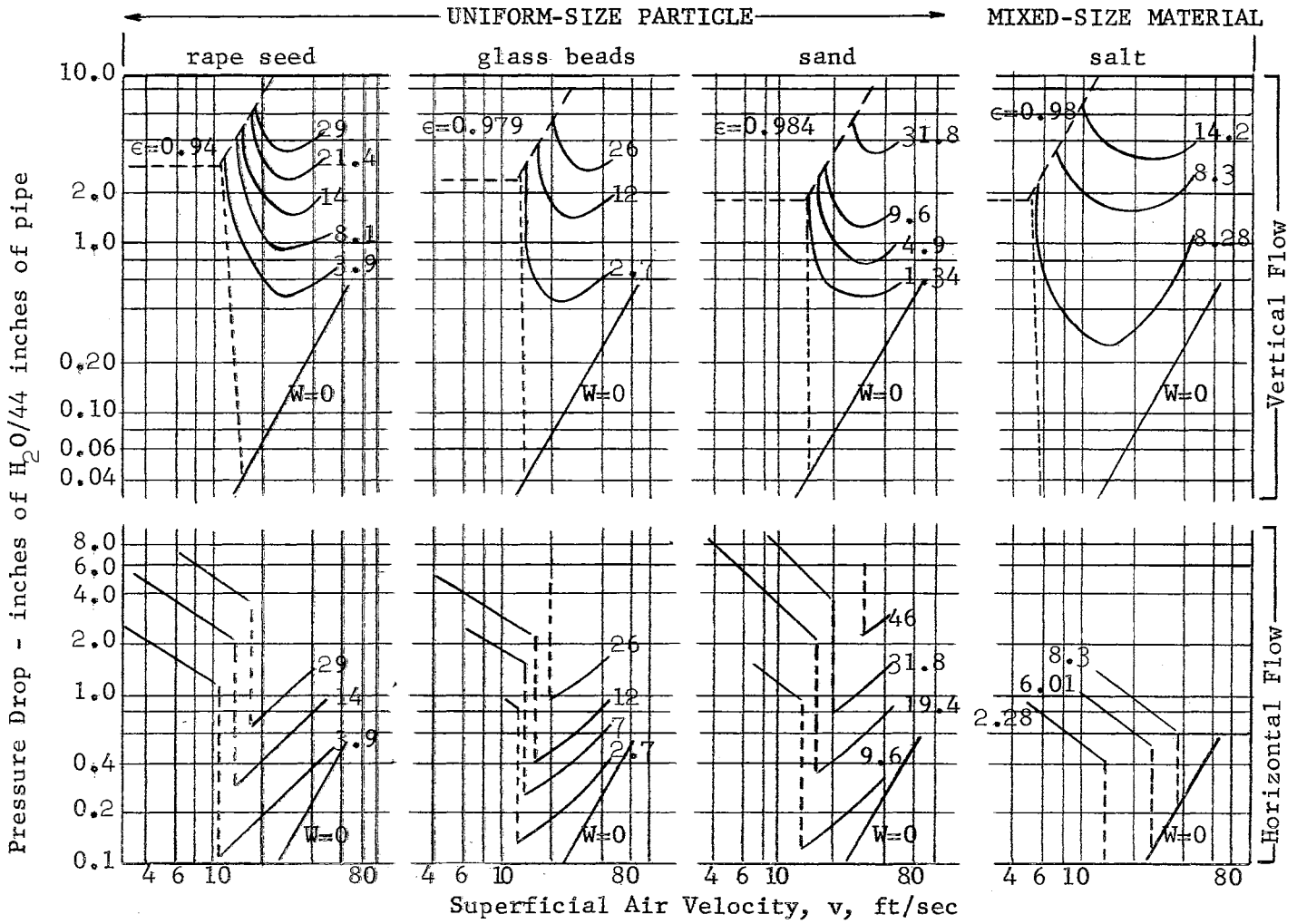

Figure 2. Experimental Data on Vertical and Horizontal Flow of Dispersed Air-Solids Suspensions in a 1.75-Inch Inside Diameter Lucite Tube

present problem. Each of the articles presented contains a bibliography of related articles and should be checked before further research is attempted.

CHAPTER III

THE RESEARCH EQUIPMENT

Equipment was selected which would fulfill the requirements of the test and minimize experimental and human error. An attempt was made to eliminate unnecessary apparatus and to provide a simple flow system. The flow diagram of the test is shown in Figure 3.

A two stage compressor was used to maintain a pressure of 125 psig in two air storage tanks. The compressor provided a continuous supply of air at the maximum test flow rate (9.15 ft^3/min. at 14.696 psia and 100°F) without pressure variations in the test section. The air passed from the tanks through a pressure regulator which reduced the pressure to 28 psig under static conditions before entering an air filter which removed any entrained oil or water from the air stream. The flow was then measured by a rotameter with a range of 0 to 9.15 ft^3/min. at standard conditions of 14.696 psia and 100°F.

Before entering the test section, the air passed through a pressure chamber and a sand hopper tube. The pressure chamber was a 10-in. x 10-in. x 10-in. air-tight chamber constructed of 1/4-in. steel plate with a 6-in. diameter viewing window of 1/4-in. plate glass. The chamber was used to determine the time of any solid particle fallout during a test run. A thermometer was located in

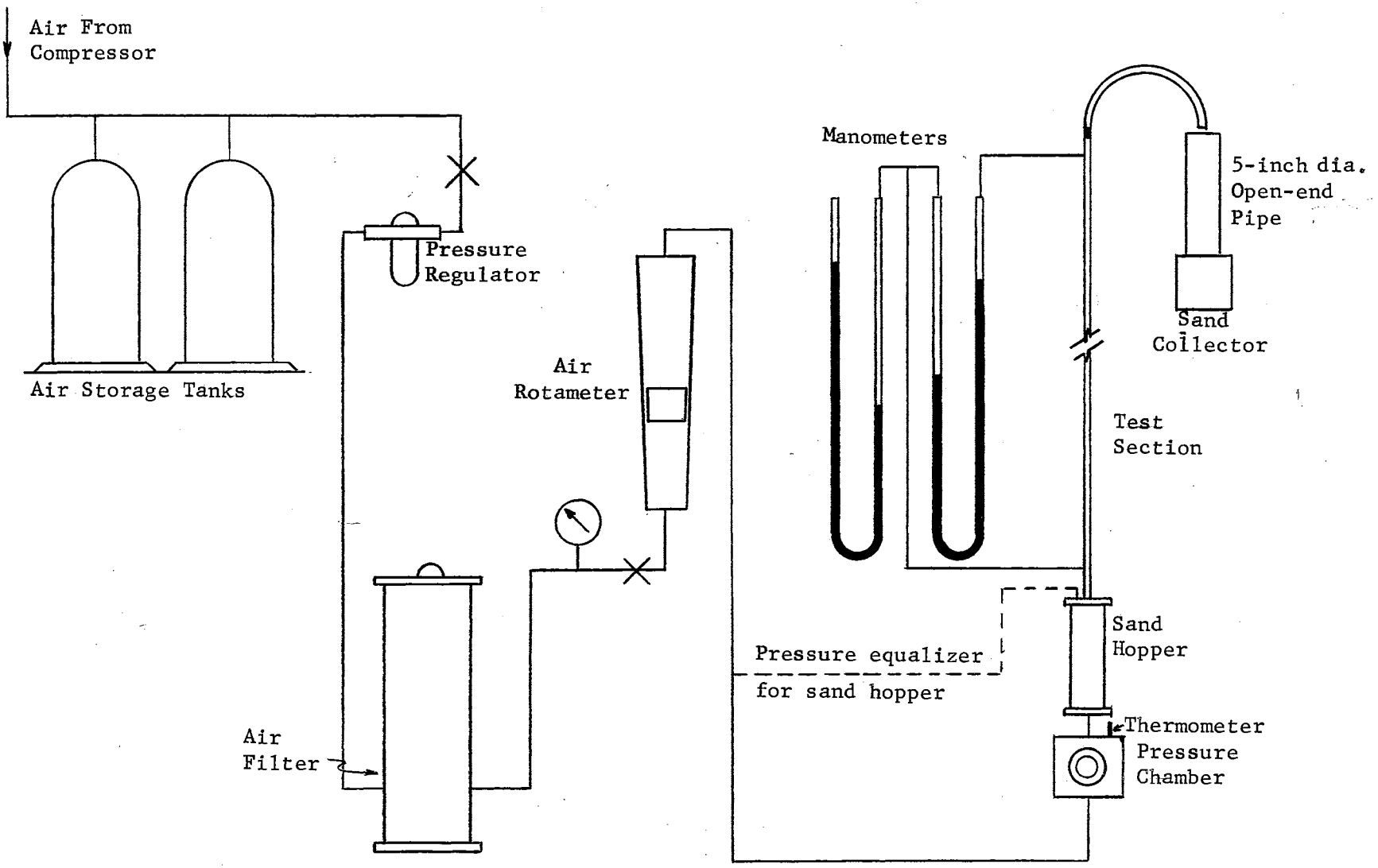

Figure 3. Diagram of Test Apparatus

the chamber to measure the temperature of the flow stream.

The sand hopper is shown in Figure 4. Its purpose was to introduce the solid particles into the air stream. The top and bottom of the hopper were constructed from 5-in. aluminum bar stock and the hopper cylinder from a 1-ft. section of 4-in. O. D. lucite tubing. The flow tube through the hopper was a 3/8-in. brass tube with an I. D. of 0.300-inch. Four slots were milled into the tube for injection of the solid particles. The slots were 3/32-in. wide and 1-in. long. The solid injection rate was controlled by variation of the slot opening by raising and lowering the hopper assembly on the brass tube using the adjustment screw shown in the figure. The hopper was filled through the 1/2-in. opening in the top. This opening was then plugged to seal the hopper assembly. A 1/4-in. rubber hose was connected from the pressure tap on the hopper to a tap located at the rotameter exit to equalize the pressure behind the sand and in the flow tube. If any air flow occurred through the sand and into the test section, it was measured air which had already passed through the rotameter. A small vibrator was attached to the hopper to insure a constant flow of the dry sand.

The test section was a 12-ft. section of pyrex tubing which had an inside diameter of 0.301-inch and an outside diameter of 0.500-inch. Pressure taps were located 10-ft. apart, one foot from either end, thus giving 40 pipe diameters of undisturbed flow both before and after the taps. The test section was mounted in a vertical position and in line with the sand hopper flow tube.

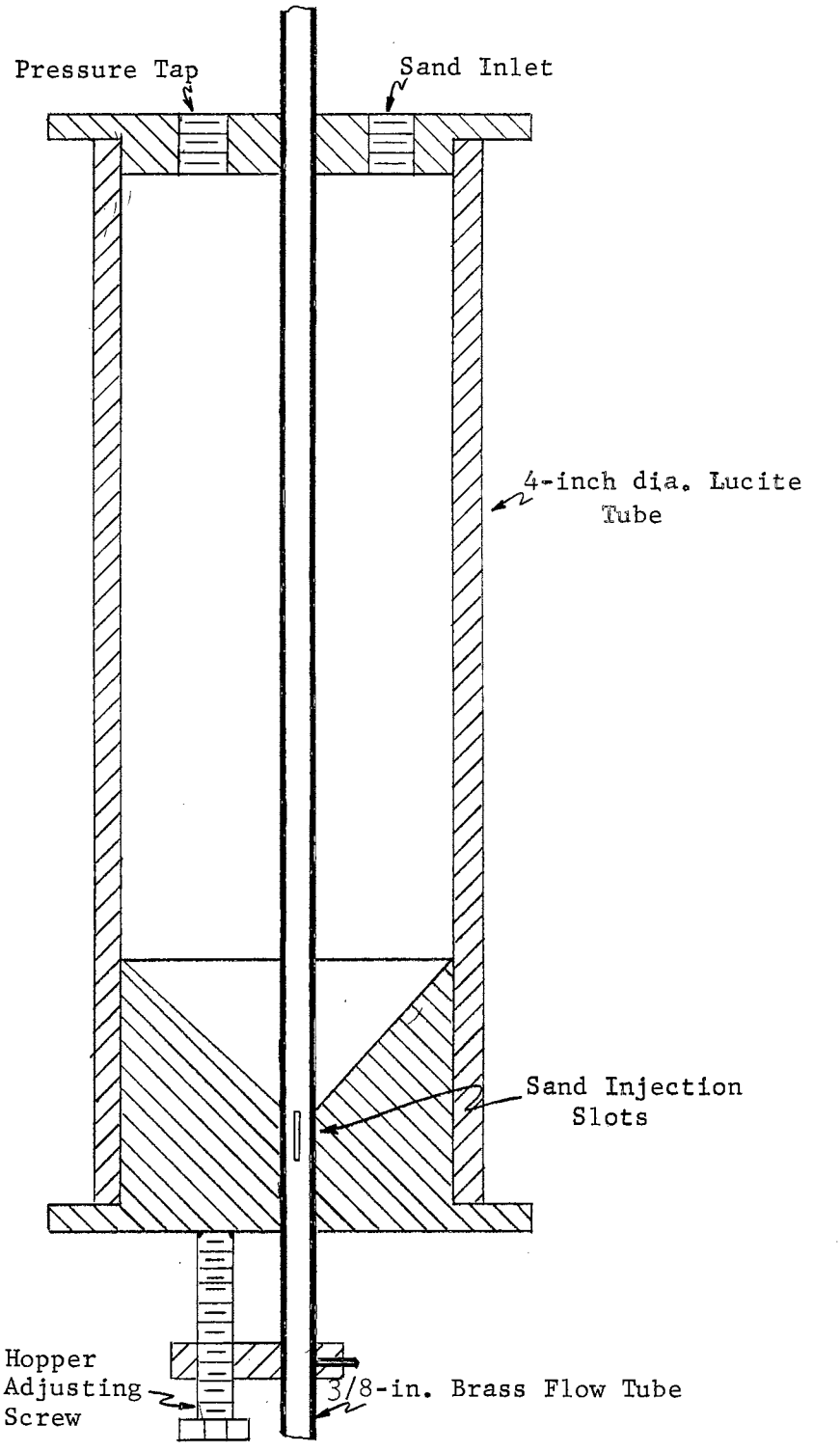

Scale: ½ inch = 1 inch

Figure 4. Sand Injection Hopper (Elevation Cross Section)

A semi-circular section of 1/2-in. copper tubing was connected at the top of the pyrex tube to direct the flow into either of two 2-ft. sections of 5-in. open-end pipe thus reducing the flow velocity and allowing the sand particles to fall into the collecting containers at the bottom of the pipes. The copper tubing was connected with a swivel joint so that the flow could be directed into either of the collectors by moving the exit.

All seals in the hopper and between brass and glass or copper and glass were obtained by using O-rings.

Two manometers were connected as shown in Figure 3 to measure the pressure at the lower pressure tap and the pressure drop in the test section. Globe valves were used to control the flow.

An equipment list is included in Appendix I.

CHAPTER IV

TEST PROCEDURE

The two stage compressor was started and time was allowed for the pressure in the air storage tanks to reach 125 psig. The flow line valves were then opened and air passed through the test section until equilibrium existed as indicated by the thermometer and manometer readings. Room temperature and the barometer reading were recorded. The flow system was checked for air leaks and instruments were inspected to insure proper operation.

Tests were run by initially adjusting the flow as recorded by the rotameter to a specified value, Q_{gs}, and then taking the required data for air flow only after equilibrium had been established. The sand hopper tube was graduated so that five different sand flow rates could be directed into the air stream. With a flow of Q_{gs} still passing through the rotameter, the hopper was adjusted to positions 1 through 5 respectively, and data was taken at each successive adjustment. The system was returned to air flow conditions after each adjustment to insure a constant Q_{gs} throughout the 5 positions. Data was not taken using all 5 positions in some of the test runs because of limitations of the equipment. The maximum rate of sand injection was limited by the hopper system and this maximum was reached before the last adjustment in some runs. The introduction

of the sand into the flow stream increased flow resistance and caused the rotameter reading to decrease and this new reading was recorded for each sand rate as Q_{2s}. After the runs for the various sand rates had been made (maintaining Q_{gs} at its initial value), Q_{gs} was reduced and additional runs were made at this new Q_{gs}. The Q_{gs} values which were used during the test ranged from 9.15 to 5.00 ft^3/min.

For each test run, equilibrium was reached in the flow stream before any data was recorded. After this equilibrium was established, the 2-phase flow stream was directed into a clean collecting container and a timer was started. At the end of the run, the stream was moved to the second collector and the time of the run recorded. The weight of sand collected during the run was recorded as W. Readings of pressure at the lower pressure tap in the pyrex tube, pressure drop in the test section, temperature of the flow stream, Q_{gs}, and Q_{2s} were taken during each run.

Since there was only a small difference in the flow stream temperature and room temperature, it was assumed that isothermal flow existed. The room temperature and barometer reading were checked frequently during the test.

The calibration curve for the rotameter is shown in Appendix II.

CHAPTER V

COMPUTATIONS

The test data and the necessary properties and dimensionless groups computed from the initial data are given in the following chapter. The present chapter presents the equations and relationships used in obtaining this additional information.

The values of flow rate read from the rotameter were converted to various other temperature and pressure conditions by the following equation:

$$Q_1 = Q_2 (P_2 T_1 / P_1 T_2)^{\frac{1}{2}}$$

where

Q_2 = Gas flow rate as measured at P_2 and T_2 (ft^3/min.)

Q_1 = Q_2 corrected to conditions at P_1 and T_1 (ft^3/min.)

T = Absolute temperature (°R)

P = Absolute pressure (psia).

The velocity of the air stream was found by the equation:

$$v = Q_{2f}/A$$

where

v = Velocity of gas flow neglecting the effect of particles in the air stream (ft/sec.)

Q_{2f} = Air flow rate at 2-phase flow conditions (ft^3/sec.)

A = Area of flow (ft^2).

The density of the gas is expressed by the equation:

$$\rho_g = (P)/(zRTg_c)$$

where

ρ_g = Gas mass density (lb_f-sec^2/ft^4)

P = Absolute pressure (lb_f/ft^2)

z = Gas compressibility factor

R = Gas constant ($ft\text{-}lb_f/lb_m\text{-}°R$)

T = Absolute temperature (°R)

g_c = 32.174 (lb_m-ft)/(lb_f-sec^2).

The weight rate of air flow was found by the equation:

$$\dot{w}_g = (\rho_g)(Q_{2f})(g)$$

where

$\dot{w}_g$ = Weight rate of air flow (lb/min.)

ρ_g = Gas mass density (lb_f-sec^2/ft^4)

Q_{2f} = Air flow rate at 2-phase flow conditions (ft^3/min.)

g = Local acceleration due to gravity (32.2 ft/sec^2).

The weight rate of particle flow was found by the equation:

$$\dot{w}_p = W/\text{Time}$$

where

$\dot{w}_p$ = Weight rate of solid flow during the test run (lb/min.)

W = Weight of solids collected during the test run (lb.)

Time = Time elapsed during the test run (min.).

The Reynolds number was determined by the equation:

$$N_R = vD\rho_g/\mu$$

where

N_R = Reynolds number

v = Air velocity (ft/sec.)

ρ_g = Gas mass density (lb_f-sec^2/ft^4)

D = Tube diameter (ft.)

μ = Absolute viscosity of the air (lb_f-sec/ft^2).

The density of the solid particles was determined, by the water displacement method, to be 5.114 (lb_f-sec^2/ft^4).

Since air was the only gas used and the temperature and cross sectional area were constant throughout the test, the following values were constant in the computations:

$A = 4.94 \times 10^{-4}$ ft^2.

$\mu = (3.83 \times 10^{-7})(lb_f\text{-}sec/ft^2)$.

$D = 0.02508$ ft.

$R = 53.35$ (ft-lb/lb_m-°R)

$z = 0.9998$

The sand particles used in the test were of random size from 28 to 35 mesh Tyler. This is a diameter range between 420 and 590 microns, or less than 1/13 of the flow-tube diameter. The sand was high-grade "frac" sand obtained from Halliburton Oil Well Cementing Company.

CHAPTER VI

TEST DATA AND RESULTS

A total of thirty four tests were run for 2-phase flow. The data recorded during the test runs are shown in Tables III and IV. Tables V through VIII list the additional information calculated from this initial test data. Information necessary for a plot of $(\Delta P/\Delta P_g)$ vs. $(\dot{w}_p/\dot{w}_g)(\rho_g/\rho_p)(N_R)_g$ is presented in these tables. Since it was necessary to determine ΔP_g for the test flow rate Q_{2s}, a plot was made of Q_{ga} vs. ΔP_g. This curve is shown in Figure 5. Values of Q_{2s} were converted to air flow conditions, Q_{2a}, and values of ΔP_g for $Q_{2a} = Q_{ga}$ were read from the curve. This procedure would not have been possible if the pressure had been varied at the exit of the test section. These values of ΔP_g from the curve are shown in Table VII.

The various flow rates listed in the tables have the following meanings:

Q_{gs} = Rotameter reading for air flowing alone (cubic ft./min. at 14.696 psig and 100°F)

Q_{ga} = Q_{gs} corrected for conditions existing during flow of air only (cubic ft./min. at T_a and P_a)

Q_{2s} = Rotameter reading for 2-phase flow (cubic ft./min. at 14.696 psia and 100°F)

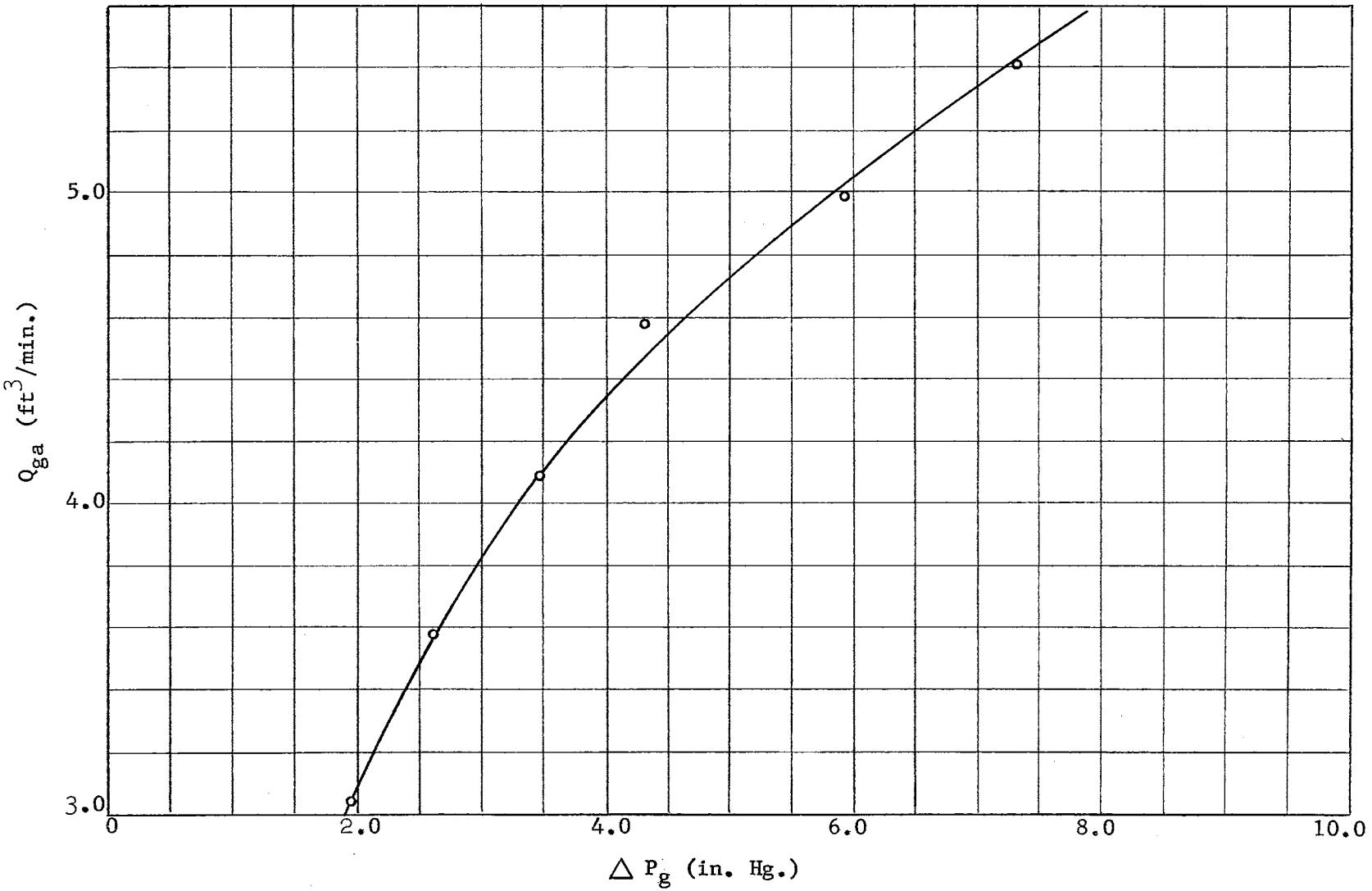

Figure 5. Relation of Q_{ga} to $\triangle P_g$ for Test Runs

TABLE III

DATA FOR AIR FLOW ONLY

Q_{gs} (ft^3/min.)	P_g (in. Hg. abs.)	ΔP_g (in. Hg.)
5.00	34.20	4.30
5.58	35.95	5.90
6.19	37.60	7.30
6.80	39.45	8.80
7.38	41.45	10.60
7.93	44.15	12.75
8.56	46.65	14.80
9.15	49.95	17.60

Barometer: 29.35 in. Hg.

Room Temperature: $80^{o}F$

T_g: $77^{o}F$

TABLE IV

DATA FOR TWO-PHASE FLOW

Run No.	Q_{2s} (ft^3/min.)	P (in. Hg. abs.)	Δ P (in. Hg.)	Time (min.)	W (lb.)
1	4.10	42.65	10.60	1.002	1.492
2	3.99	43.15	10.90	1.002	2.188
3	3.86	43.85	11.50	1.014	2.523
4	4.65	44.05	11.60	1.003	1.391
5	4.35	46.45	13.20	0.998	2.438
6	4.23	47.05	13.60	1.001	3.141
7	4.23	47.45	13.90	1.003	3.406
8	5.00	46.35	13.10	1.002	1.578
9	4.70	48.75	14.70	1.001	2.609
10	4.58	49.85	15.40	1.005	3.336
11	4.52	50.05	15.70	1.002	3.563
12	5.30	49.25	14.90	1.004	2.109
13	4.88	51.65	16.50	1.002	3.188
14	4.76	52.45	17.10	1.003	3.500
15	4.76	52.55	17.20	0.805	3.234
16	5.72	50.95	16.20	1.003	1.859
17	5.30	53.65	17.90	1.002	2.875
18	5.07	54.45	18.30	0.919	3.406

TABLE IV (CONTINUED)

Run No.	Q_{2s} (ft^3/min.)	P (in. Hg. abs.)	ΔP (in. Hg.)	Time (min.)	W (lb.)
19	5.00	54.65	18.50	0.815	3.313
20	5.90	54.05	18.30	1.002	2.281
21	5.30	56.70	19.90	0.956	3.266
22	5.25	57.05	20.10	0.863	3.328
23	5.19	57.15	20.10	0.815	3.328
24	5.12	57.15	20.10	0.788	3.313
25	6.25	56.75	20.20	1.001	2.375
26	5.58	58.95	21.30	0.862	3.109
27	5.36	59.55	21.80	0.763	3.125
28	5.30	59.65	21.90	0.706	3.063
29	5.30	59.45	21.60	0.714	3.125
30	6.55	58.15	21.70	1.004	2.438
31	5.72	60.95	23.40	1.002	3.656
32	5.58	61.75	23.60	0.822	3.328
33	5.42	61.95	23.40	0.749	3.281
34	5.42	61.35	23.00	0.836	3.594

Barometer: 29.35 in. Hg.

Room Temperature: $80^{\circ}F$

$T_g = T$: $437^{\circ}R$

TABLE V

DATA FOR Q_{ga} vs. ΔP_g CURVE

Q_{ga} (ft^3/min.)	P_g (psia)	ΔP_g (in. Hg.)
3.051	15.50	1.95
3.581	15.87	2.60
4.088	16.33	3.45
4.579	16.80	4.30
4.985	17.66	5.90
5.407	18.47	7.30
5.799	19.38	8.80
6.140	20.36	10.60
6.392	21.69	12.75
6.714	22.91	14.80
6.934	24.54	17.60

TABLE VI

FLOW STREAM PROPERTIES

Run No.	Q_{2a} (ft^3/min.)	Q_{2f} (ft^3/min.)	v (ft/sec)	ρ_g (slugs/ft^3)	$\dot{w}_g$ (lb/min.)	$\dot{w}_g$ (lb/min.)
1	3.755	3.363	113.4	3.20×10^{-3}	0.347	1.489
2	3.654	3.253	109.7	3.24	0.339	2.184
3	3.535	3.122	105.3	3.29	0.331	2.488
4	4.154	3.752	126.5	3.31	0.400	1.387
5	3.886	3.418	115.3	3.49	0.384	2.443
6	3.779	3.303	111.4	3.53	0.376	3.138
7	3.779	3.289	110.9	3.56	0.377	3.396
8	4.367	3.933	132.6	3.48	0.441	1.575
9	4.105	3.605	121.6	3.66	0.425	2.606
10	4.000	3.474	117.2	3.74	0.419	3.319
11	3.948	3.422	115.4	3.76	0.414	3.556
12	4.520	4.046	136.4	3.70	0.482	2.101
13	4.162	3.637	122.7	3.88	0.454	3.182
14	4.059	3.521	118.7	3.94	0.446	3.490
15	4.059	3.518	118.6	3.95	0.447	4.017
16	4.759	4.292	144.8	3.83	0.529	1.853
17	4.410	3.876	130.7	4.03	0.503	2.869
18	4.218	3.680	124.1	4.09	0.485	3.706
19	4.160	3.623	122.2	4.10×10^{-3}	0.479	4.065

TABLE VI (CONTINUED)

Run	Q_{2a} (ft^3/min.)	Q_{2f} (ft^3/min.)	v (ft/sec)	ρ_g (slugs/ft^3)	$\dot{w}_g$ (lb/min.)	$\dot{w}_g$ (lb/min.)
20	4.756	4.298	145.0	4.06×10^{-3}	0.562	2.276
21	4.272	3.770	127.1	4.26	0.517	3.416
22	4.232	3.724	125.6	4.28	0.514	3.856
23	4.184	3.677	124.0	4.29	0.508	4.083
24	4.127	3.628	122.4	4.29	0.501	4.204
25	4.902	4.444	149.9	4.26	0.610	2.373
26	4.377	3.893	131.3	4.43	0.555	3.607
27	4.204	3.721	125.5	4147	0.536	4.096
28	4.157	3.676	124.0	4.48	0.530	4.339
29	4.157	3.682	124.2	4.46	0.529	4.377
30	4.963	4.601	155.2	4.37	0.647	2.428
31	4.334	3.924	132.3	4.58	0.578	3.649
32	4.228	3.804	128.3	4.64	0.568	4.049
33	4.107	3.689	124.4	4.65	0.553	4.381
34	4.107	3.706	125.0	4.61×10^{-3}	0.550	4.300

TABLE VII

DETERMINATION OF $(\Delta P/\Delta P_g)$

By use of Figure 5

Run No.	Q_{2a} (ft^3/min.)	ΔP_g (in. Hg.)	ΔP (in. Hg.)	$(\Delta P/\Delta P_g)$
1	3.755	2.87	10.60	3.693
2	3.654	2.70	10.90	4.037
3	3.535	2.55	11.50	4.510
4	4.154	3.51	11.60	3.305
5	3.886	3.06	13.20	4.314
6	3.779	2.90	13.60	4.690
7	3.779	2.90	13.90	4.793
8	4.367	3.96	13.10	3.308
9	4.105	3.45	14.70	4.261
10	4.000	3.25	15.40	4.738
11	3.948	3.16	15.70	4.968
12	4.520	4.31	14.90	3.457
13	4.162	3.55	16.50	4.648
14	4.059	3.35	17.10	5.104
15	4.059	3.35	17.20	5.134
16	4.759	5.01	16.20	3.234
17	4.410	4.05	17.90	4.420
18	4.218	3.66	18.30	5.000

TABLE VII (CONTINUED)

Run No.	Q_{2a} (ft^3/min.)	ΔP_g (in. Hg.)	ΔP (in. Hg.)	$(\Delta P/\Delta P_g)$
19	4.160	3.55	18.50	5.211
20	4.756	5.01	18.30	3.653
21	4.272	3.76	19.90	5.293
22	4.232	3.69	20.10	5.447
23	4.184	3.58	20.10	5.615
24	4.127	3.49	20.10	5.759
25	4.902	5.45	20.20	3.706
26	4.377	4.00	21.30	5.325
27	4.204	3.61	21.80	6.039
28	4.157	3.55	21.90	6.169
29	4.157	3.55	21.60	6.085
30	4.963	5.65	21.70	3.841
31	4.334	3.90	23.40	6.000
32	4.228	3.68	23.60	6.413
33	4.107	3.45	23.40	6.783
34	4.107	3.45	23.00	6.667

TABLE VIII

DIMENSIONLESS GROUPS

Run No.	$(\dot{w}_p/\dot{w}_g)$	(ρ_g/ρ_p)	$(N_R)_g$	$(\frac{\dot{w}_p}{\dot{w}_g})(\frac{\rho_g}{\rho_p})(N_R)_g$
1	4.295	6.26×10^{-4}	23,783	63.95
2	6.435	6.34	23,279	94.98
3	7.519	6.44	22,696	109.90
4	3.472	6.47	27,398	61.54
5	6.364	6.82	26,331	114.28
6	8.352	6.91	25,761	148.67
7	9.001	6.97	25,879	162.36
8	3.574	6.81	30,227	73.57
9	6.132	7.16	29,147	127.98
10	7.927	7.32	28,714	166.63
11	8.589	7.35	28,393	179.25
12	4.363	7.23	33,036	104.20
13	7.006	7.58	31,150	165.44
14	7.818	7.70	30,613	184.29
15	8.989	7.71	30,646	212.41
16	3.504	7.48	36,265	95.05
17	5.708	7.88	34,470	155.05
18	7.649	8.00×10^{-4}	33,233	203.35

TABLE VIII (CONTINUED)

Run No.	$(\dot{w}_p/\dot{w}_g)$	(ρ_g/ρ_p)	$(N_R)_g$	$(\frac{\dot{w}_p}{\dot{w}_g})(\frac{\rho_g}{\rho_p})(N_R)_g$
19	8,495	8.02×10^{-4}	32,820	223.60
20	4.053	7.94	38,517	123.95
21	6.610	8.33	35,439	195.13
22	7.508	8.38	35,223	221.63
23	8.039	8.39	34,837	234.98
24	8.388	8.39	34,372	241.91
25	3.892	8.33	41,818	135.57
26	6.501	8.66	38,052	214.23
27	7.646	8.74	36,743	245.55
28	8.187	8.76	36,350	260.70
29	8.273	8.73	36,291	262.09
30	3.754	8.54	44,352	142.19
31	6.311	8.95	39,657	223.98
32	7.130	9.07	38,949	251.89
33	7.929	9.10	37,889	273.37
34	7.821	9.01×10^{-4}	37,705	265.71

Q_{2a} = Q_{2s} corrected for conditions existing during flow of air only (cubic ft./min. at T_a and P_a)

Q_{2f} = Q_{2s} corrected for conditions existing during 2-phase flow (cubic ft./min. at T and P).

It must be remembered that ΔP_g and $(N_R)_g$ are for conditions of gas flow only. Figure 6 shows the plot of the test results.

A preliminary test was run to determine if the test setup would yield results for air flow alone which could be predicted by previously used methods. Test data and calculated data are presented in Appendix III for a test using air only. The resulting curve is compared to the Moody friction factor diagram. The curves compare satisfactorily.

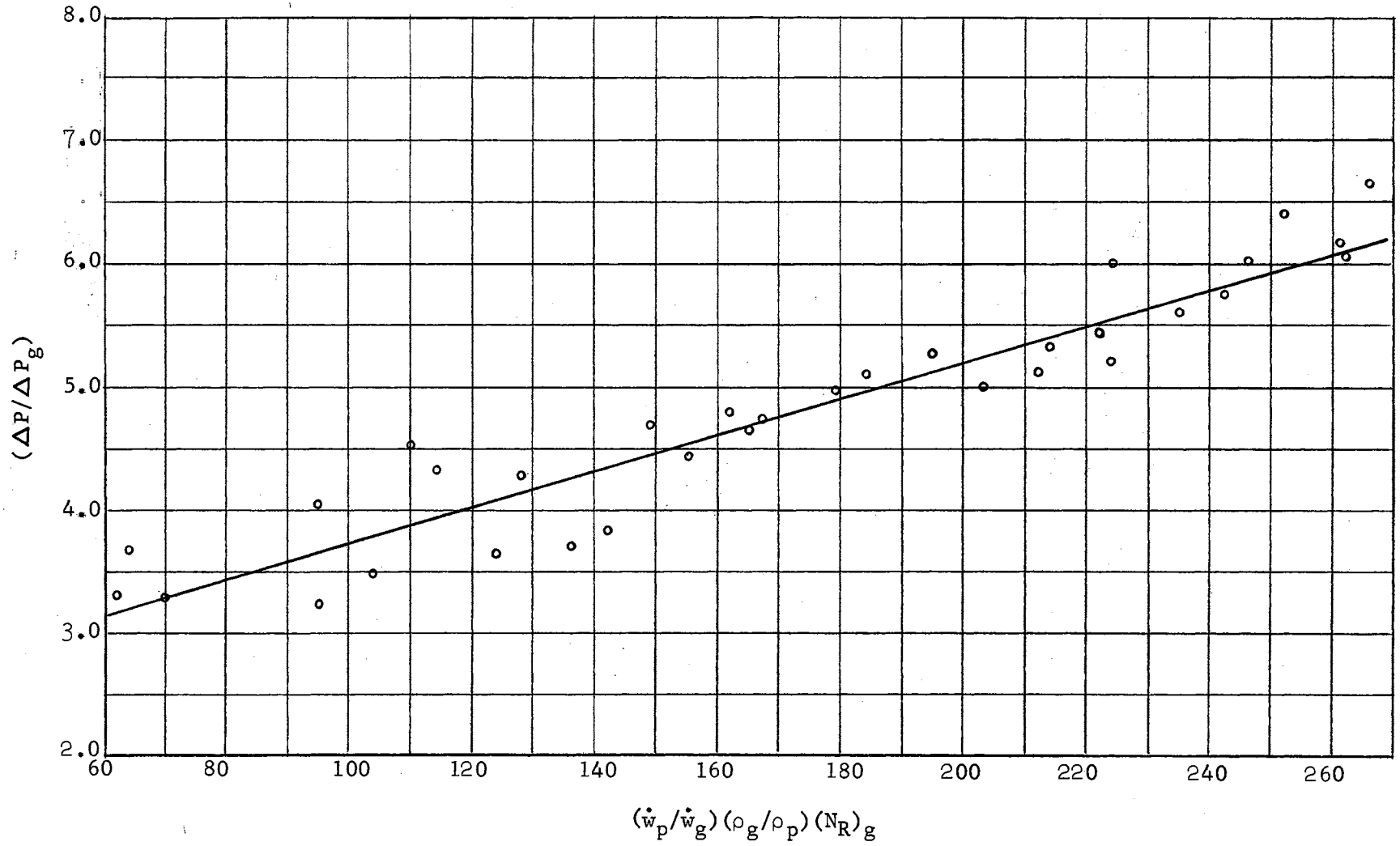

Figure 6. Relation Between $(\Delta P/\Delta P_g)$ and $(\dot{w}_p/\dot{w}_g)(\rho_g/\rho_p)(N_R)_g$

CHAPTER VII

ANALYSIS OF RESULTS

The curve of $(\Delta P/\Delta P_g)$ vs. $(\dot{w}_p/\dot{w}_g)(\rho_g/\rho_p)(N_R)_g$ is shown in Figure 6. The data, although somewhat scattered, is well correlated by these parameters and can be approximated by a straight line. This indicates that the ratio, $(\Delta P/\Delta P_g)$, can be represented by the linear relationship

$$(\Delta P/\Delta P_g) = K(\dot{w}_p/\dot{w}_g)(\rho_g/\rho_p)(N_R)_g + C$$

where K and C are constants and the remaining terms are dimensionless groups. The least square method was applied to the data points and a linear approximation was obtained. Values for K and C were found to be 0.0152 and 2.213, respectively. Therefore, it follows that the ratio $(\Delta P/\Delta P_g)$, within the range of this study, can be predicted by the relationship

$$(\Delta P/\Delta P_g) = 0.0152(\dot{w}_p/\dot{w}_g)(\rho_g/\rho_p)(N_R)_g + 2.213.$$

It should be mentioned that the product $(\dot{w}_p/\dot{w}_g)(\rho_g/\rho_p)(N_R)_g$ can be expressed as $(\dot{w}_p/\rho_g vAg)(\rho_g/\rho_p)(vD\rho_g/\mu)$ which equals $(D/\mu)(1/\rho_p Ag)(\rho_g \dot{w}_p)$. D, μ, ρ_p, A, and g are all constant for the test runs. Therefore, ρ_g and $\dot{w}_p$ were the only variables for these tests. ρ_g can be determined with little error if pressure and temperature readings are carefully taken and the value varies only a small amount throughout the range of tests. The only remaining data recorded are those leading to values of $\dot{w}_p$. Thus it is necessary to obtain accurate values of this factor if the test results are to

be valid. The solids transported during these tests ranged from 3.472 pounds of solid per pound of gas to 9.001 pounds of solid per pound of gas. No previous work was available which could be used to check the experimental results of the tests.

The straight line relationship has a positive slope which is constant throughout the test range. It is recommended that future tests be run to determine the maximum value of $(\Delta P/\Delta P_g)$ and $(\dot{w}_p/\dot{w}_g)(\rho_g/\rho_p)(N_R)_g$ obtained before the curve has a definite change in slope. Qualitative reasoning makes it clear that an upper limit to these flow parameters must exist since $\dot{w}_p$ obviously cannot increase without limit. These tests will require a change in equipment from that used in the present tests to allow either (a) accurate measurement of small values of $\dot{w}_g$ or (b) an increased gas density, ρ_g.

The results presented in this report are dependent on size of solid particles injected into the flow stream. Since the drag on the particles increases approximately as the square of the diameter and the gravity force increases as the cube of the diameter, it is believed that the straight line in Figure 6 would have had a greater positive slope if larger particles had been used and a smaller positive slope if smaller particles had been used. Tests should be run to determine the effect of particle size on the constants K and C.

CHAPTER VIII

CONCLUSIONS AND RECOMMENDATIONS

Test equipment was designed and assembled which can be used to determine the pressure drop in two-phase (gas-solid) flow. A free-flow hopper was used to inject the solids into the flow stream at a uniform rate. This method proved satisfactory and permits negligible fluctuations in pressure readings during a test run. The test data could be reproduced within very narrow limits.

The pressure drop which occurs during vertically upward, isothermal, gas-solid flow can be predicted by

$$(\Delta P/\Delta P_g) = 0.0152(\dot{w}_p/\dot{w}_g)(\rho_g/\rho_p)(N_R)_g + 2.213$$

where

ΔP = Pressure drop in the test section for two-phase flow

ΔP_g = Pressure drop in the test section for the gas flowing alone (No solids)

$\dot{w}_p$ = Weight rate of solid particles (lb/min.)

$\dot{w}_g$ = Weight rate of gas (lb/min.)

ρ_g = Mass density of the gas during two-phase flow (lb_f-sec^2/ft^4)

ρ_p = Mass density of the solid particles (lb_f-sec^2/ft^4)

$(N_R)_g$ = Reynolds number of the gas flowing alone.

The range of values used in the tests was:

$\dot{w}_p$: 1.387 to 4.377 lb/min.

$\dot{w}_g$: 0.331 to 0.647 lb/min.

$(N_R)_g$: 22,700 to 44,350.

Air was used as the gas and sand particles with a diameter range of 420 to 590 microns as the solid. The diameter of the test section was 0.301 inch.

It is recommended that further tests be run using increased values of $(\dot{w}_p/\dot{w}_g)(\rho_g/\rho_p)(N_R)_g$ and various solid particle diameters.

BIBLIOGRAPHY

1. Happel, J., "Viscosity of Suspensions of Uniform Spheres," J. Applied Physics, vol. 28, no. 11, November 1957, pp 1288-1292.

2. Croft, H. O., Thermodynamics Fluid Flow and Heat Transmission, McGraw-Hill Company, Inc., New York and London (1938).

3. Alves, G. E., "Cocurrent Liquid-Gas Flow in Pipe Line Contactor," Chem. Engr. Progress, vol. 50, no. 9, September 1954, pp 449-456.

4. Hariu, O. H. and Molstad, M. C., "Pressure Drop in Vertical Tubes in Transport of Solids by Gases," Ind. Engr. Chem., vol. 41, no. 6, June 1949, pp 1148-1160.

5. Wilhelm, R. H. and Kwauk, M., "Fluidization of Solid Particles," Chem. Engr. Progress, vol. 44, 1948, p 201.

6. Hazen, A., Hardy, E. D., and Blatch, Nora S., "Works for the Purification of the Water Supply of Washington D. C.," Trans. ASCE, 1906, 57, 307.

7. Alden, J. L., "Industrial Exhaust Ventilation--Low Pressure Pneumatic Conveying Systems," Heating and Ventilating, August 1938, pp 30-34.

8. Soo, S. L., Ihrig, H. K. Jr., and El Kouh, A. F., "Experimental Determination of Statistical Properties of Two-Phase Turbulent Motion," Paper No. 59--A-59, ASME, 1959.

9. Zenz, F. A., "Two-Phase Fluid-Solid Flow," Ind. Engr. Chem., vol. 41, no. 12, December 1949, pp 2801-2806.

APPENDIX I

LIST OF EQUIPMENT

1 - Fischer and Porter rotameter #B-851346; 0-8.5 cfm air at 0 psig and 100°F; tube #5A-25; 3/4-in. pipe inlet and outlet.

1 - Commercial Filters Corporation fulflow filter; Model WF6; 2-in. pipe inlet and outlet; cotton packing.

1 - Fisher Governor Company pressure regulator; Type 630; Serial no. 2035007; maximum inlet pressure, 1000 psi; maximum outlet pressure, 30 psi.

1 - Meriam Instrument Company manometer bank; Type W; Model M-202; Serial no. G50801; 0-50-in. Hg. range.

1 - Standard Electric timer; Type S-6; No. 44655; 0.001 to 10.000 minute range.

1 - Troemner beam balance scale; Type 19; Serial no. W2; No. 124; 16 lb. capacity.

1 - Standard 6-inch mercury thermometer; -20 to +120°F range.

1 - Mastergauge pressure gauge; Type 101; 0-200 psi range.

The air was supplied by a Pennsylvania Pump and Compressor Company two-stage air compressor; Serial no. 4727; Class 11AT; Rated at 100 cfm at 400 rpm. The compressor was driven by a 25 hp electric motor.

APPENDIX II

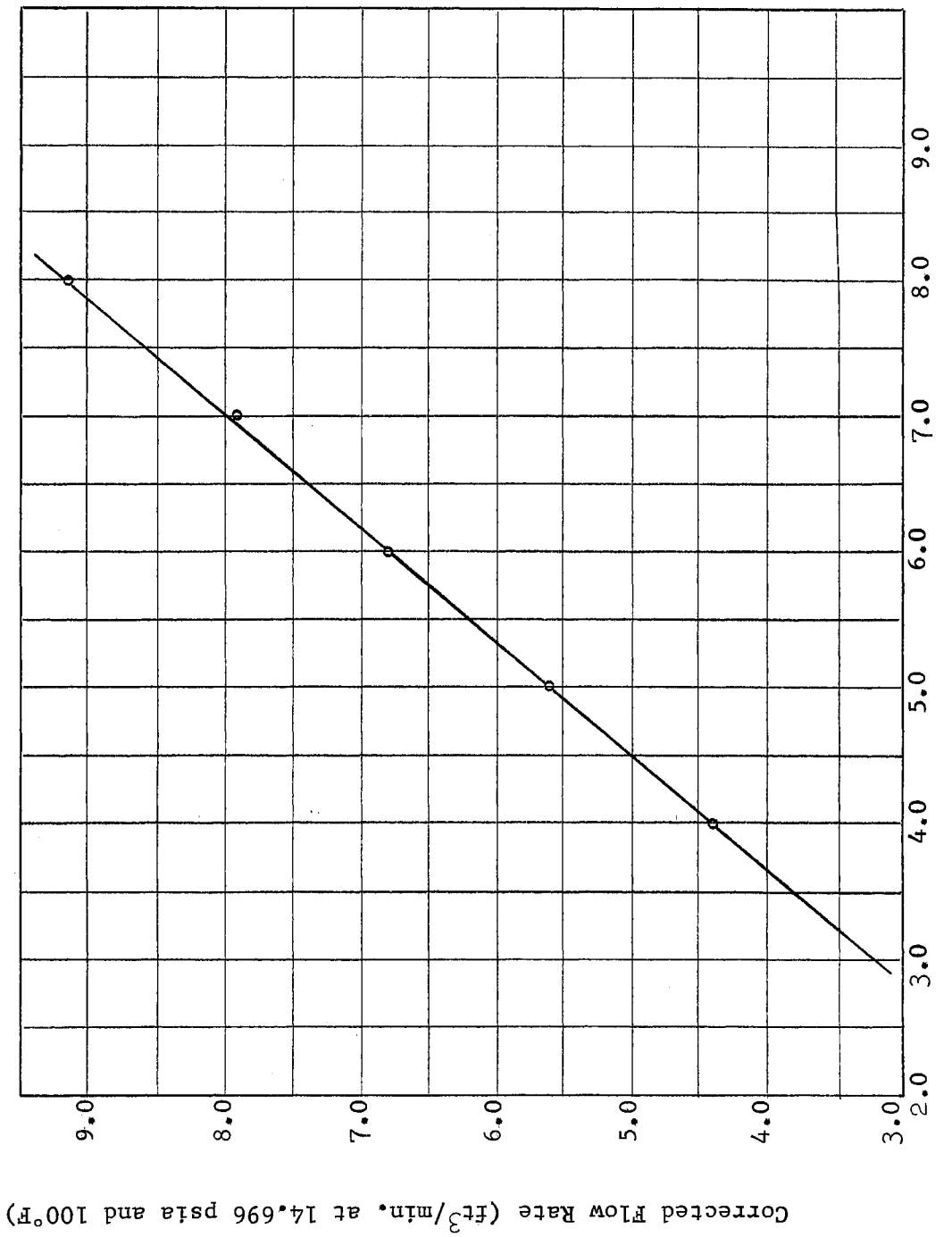

Figure 7. Rotameter Calibration Curve

APPENDIX III

COMPARISON OF TEST DATA WITH MOODY DIAGRAM RESULTS

A preliminary test run was made using air only, to check the reliability of the test apparatus. Experimental data was taken and values of friction factor, f, and Reynolds number, N_R, were calculated. These calculated values were plotted on the Moody Diagram and were found to compare satisfactorily as shown in Figure 8. The test data and calculated data are shown in Tables IX and X respectively. The glass test section was smooth when these runs were made but became very rough after the tests using sand in the air stream.

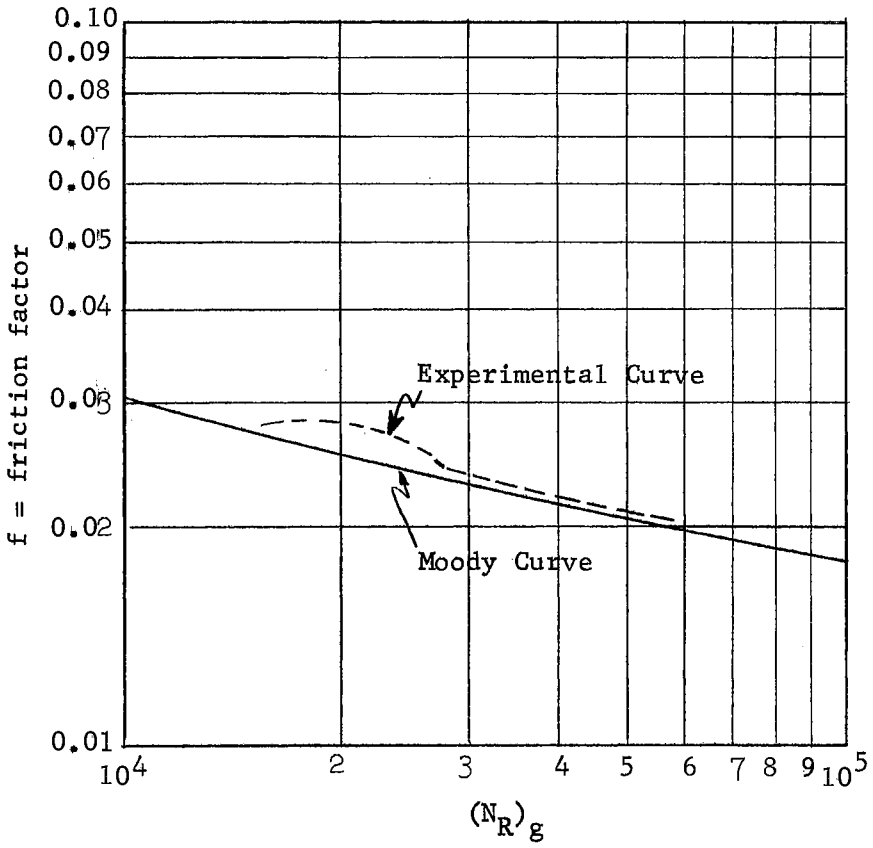

Figure 8. Comparison of the Test Data With the Moody Diagram

TABLE IX

EXPERIMENTAL DATA FOR CHECK OF TEST EQUIPMENT

Run No.	Q_{gs} (ft^3/min.)	P (in. Hg. gauge)	ΔP (in. Hg.)	T_g (^oR)
1	3.20	2.60	2.00	549
2	3.80	3.82	2.90	549
3	4.40	5.10	3.70	549
4	5.00	6.70	4.35	549
5	5.58	8.63	5.20	549
6	6.19	9.95	6.25	549
7	6.80	11.20	7.25	549
8	7.38	13.20	8.40	549
9	7.93	15.10	9.45	549
10	8.56	17.60	10.85	549
11	9.15	19.95	12.05	549

Date: 6/29/60

Barometer Reading: 29.15 in. Hg.

Room Temperature: 95°F

TABLE X

CALCULATED DATA FOR CHECK OF TEST EQUIPMENT

Q_{ga} (ft^3/sec)	v (ft/sec)	ρ_g ($16\ -sec^2/ft^4$)	N_R	f
0.0513	103.7	2.38×10^{-3}	15,942	0.0279
0.0597	120.9	2.48	19,289	0.0282
0.0679	137.3	2.57	22,760	0.0272
0.0754	152.5	2.69	26,464	0.0247
0.0819	165.8	2.84	30,316	0.0237
0.0894	180.8	2.94	34,217	0.0231
0.0966	195.5	3.03	38,185	0.0222
0.1024	207.1	3.18	42,451	0.0218
0.1076	217.8	3.32	46,638	0.0213
0.1130	228.7	3.51	51,748	0.0210
0.1179	238.5	3.69×10^{-3}	56,681	0.0204

VITA

Kirk Ewell Boatright

Candidate for the Degree of

Master of Science

Thesis: TRANSPORTATION OF SOLID PARTICLES IN A GAS FLOW STREAM

Major Field: Mechanical Engineering

Biographical:

Personal Data: Born at Muskogee, Oklahoma, February 9, 1937, the son of Ewell A. and Ruth E. Boatright.

Education: Attended grade school in Fort Gibson, Oklahoma; graduated from Fort Gibson High School in 1955; received the Bachelor of Science degree from Oklahoma State University, with a major in Mechanical Engineering, in May, 1959; completed the requirements for the Master of Science degree in August, 1960.

Experience: Part-time clerk in grocery during high school; employed as a roustabout for Cities Service Oil Company in Vernon, Texas, during summer of 1958; employed as a Jr. Research Engineer at Pan American Petroleum Corporation Research Center in Tulsa, Oklahoma, during the summer of 1959.

Professional Organizations: AIME; American Society of Mechanical Engineers.

Honorary Organizations: Pi Tau Sigma; Sigma Tau; Blue Key; Phi Kappa Phi; Phi Eta Sigma.

Honors and Awards: Hamilton Award in Engineering, 1959; St. Pat Salutes Award, 1959; Who's Who in American Colleges and Universities, 1959; O.S.U. Redskin Congratulate, 1959; President of O.S.U. Student Body and Student Senate, 1958-59; Cities Service Oil Company Junior and Senior Scholarships; Pan American Petroleum Corporation Graduate Fellowship, 1959-60.